High-Resolution ^{13}C CP/MAS NMR Study on Structure and Structural Transition of *Antheraea pernyi* Silk Fibroin Containing Poly(L-alanine) and Gly-Rich Regions

Yasumoto Nakazawa and Tetsuo Asakura*

Department of Biotechnology, Tokyo University of Agriculture and Technology, Koganei, Tokyo 184-8588, Japan

Received November 15, 2001

ABSTRACT: The structure and structural transition of silk fibroin from a wild silkworm *Antheraea pernyi* (*A. pernyi*), whose amino acid sequence consists of poly(L-alanine) (PLA) and a Gly-rich region, were studied with solid-state ^{13}C cross-polarization magic angle spinning (CP/MAS) NMR. As such, there has been limited information on the inherent "conformationally flexible" Gly-rich region of *A. pernyi*, presumably due to lack of an appropriate analytical technique required to contribute for the understanding of unique structural properties. The effective use of conformation-dependent ^{13}C NMR chemical shifts of isotopically labeled silk sample may overcome such limitations and prove valuable the structural analysis. Thus, the C_α and C_β carbons of Ser residue, C_β carbon of Tyr residue, and the CO carbon of Gly residue were ^{13}C-isotope-labeled, and the conformation-dependent ^{13}C chemical shifts of these residues were used for elucidating the conformation. In the silk fibroin film prepared from the silk gland 65% of Ser residues are in the α-helical state. These Ser residues with α-helix form can be assigned to those located at the N-terminal of PLA and are considered to be incorporated into the α-helix of PLA. The Tyr and other Ser residues take the random coil form. The structural transition from α-helix to *β*-sheet in the PLA region occurs by immersing the film in 3:2 methanol−water mixture, but 20% of Ala residues still remain as an α-helix. Eighty percent of the Ser residues take the *β*-sheet, including a small amount of random coil form. The Gly carbonyl carbon peaks shift to a higher field by 1.4 ppm (172.3−170.9 ppm) when the helix to *β*-sheet transition of PLA region occurs, indicating that the structural change from random coil to *β*-sheet structure occurs in the Gly residues although the distribution in the conformation is large, as judged from the broad Gly C═O peak. Most of the Tyr residue remains as a random coil after the structural transition of the PLA region.

Introduction

Natural silks have become the subject of extensive study as model systems for high-performance biopolymers and polymer composites in part because of their impressive mechanical properties.[1] Silks are encoded by highly repetitive structural genes that are under tight regulatory control in the cell. The repetitive domains take highly ordered structure and result in fibers with unusual functional properties such as high strength and toughness. The silk fibroin from the domesticated silkworm, *Bombyx mori* (*B. mori*), is a well-known fibrous protein whose amino acid composition (in mol %) is 42.9% Gly, 30.0% Ala, 12.2% Ser, 4.8% Tyr, and 2.5% Val as listed in Table 1.[2] The complete sequence of the heavy chain has been reported by Zhou et al.[3] In addition to the well-known repeating sequence of $(GAGAGS)_n$, the repetitive region of the primary sequence of *B. mori* silk fibroin also contains the following repeating sequences: GAGAGY and GAGAGVGY. The repetitive structural region is flagged on both sides by the amorphous region with a typical sequence, TGSSGFGPYVANGGYSGYEYAWSSESDFGT, containing both polar and bulky amino acid residues. The secondary structure of the silk fibroin fiber which is named as silk II has been proposed by Marsh et al.[4] as an antiparallel *β*-sheet, based on X-ray diffraction studies and by assuming the model sequence -$(Gly\text{-}Ala)_n$-. This structural model has been supported by more detailed X-ray diffraction analyses[5,6] and IR studies[7] as well as ^{13}C and ^{15}N solid-state NMR analyses.[8−13] Most recently, the conformation of the silk fibroin film prepared from the silk fibroin stored in the silk gland of *B. mori* silkworm has been clarified by us mainly using solid-state NMR techniques. The solid-state conformation of silk I of the main sequence $(GAGAGS)_n$ was a "repeated *β*-turn type II structure".[14−16] The fiber formation mechanism could be interpreted well in terms with the structural transition from silk I to silk II.

Table 1. Amino Acid Compositions of *B. mori*, *S. c. ricini*, and *A. pernyi* Silk Fibroins (in mol %)[2]

amino acid	*B. mori*	*S. c. ricini*	*A. pernyi*
Ala	30.0	48.4	48.6
Gly	42.9	33.2	28.3
Tyr	4.8	4.5	3.7
Ser	12.2	5.5	8.9
Asp	1.9	2.7	3.9
Arg	0.5	1.7	2.6
His	0.2	1.0	0.7
Glu	1.4	0.7	0.2
Lys	0.4	0.2	0.1
Val	2.5	0.4	0.7
Leu	0.6	0.3	0.3
Ile	0.6	0.4	0.4
Phe	0.7	0.2	0.2
Pro	0.5	0.4	0.3
Thr	0.9	0.5	0.5
Met	0.1	0.0	0.0
Cys	0.0	0.0	0.0
Trp		0.3	0.5

Among silkworms, the fiber properties are considerably different among *B. mori* silk and wild silkworm silk such as *A. pernyi*, *Antheraea yamamai* (*A. yamamai*), and *Samia cynthia ricini* (*S. c. ricini*). For example, the stress−strain curve is quite different. The curve is a

10.1021/ma011999t CCC: $22.00
Published on Web 02/16/2002

Motif 1

GAGAGGAGGSYGWGDGGYGSDS
GSGAGGAGGGYGWGDDGYGSDS
GSGAGGAGGGYGWGDDGYGSDS
GSGAGGAGGGYGWGDGGYGSDS
GSGAGGAGGGYGWGDGGYGSDS
GSGAGGAGGGYGWGDGGYGSDS
GSGAGGAGGGYGWGDGGYGSDS
GSGAGGAGGGYGWGDGGYGSDS
GSGAGGAGGGYGWGDGGYGSDS
GSGAGGAGGGYGWGDGGYGSYS
GSGAGGAGGGYGWGDSGYGSDS
GSSAGGAGGGYGWGDGGYGSDS
GSSAGGAGGGYGWGDGGYGSDS
GSGAGGSGGGYGWGDGGYGSGSS
GSGAGGIGGGFGRGDGGYGSGSS

Motif 2

GSGAGGRGDGGYGSGSS
GSGAGGRGDGGYGSGSS
GSGAGGRGDGGYGSGSS
GSGAGGRGDGGYGSGSS
GSGAGGRGDGGYGSGSS
GSGAGGRGDGGYGSGSS
GSGAGGRGDGGYGSGSS
GSGAGGRGDGGYGSGSS
GSGAGGRGDGGYGSGSS
GSGAGGRGDGGYGSGSS
SSGAGGRGDGGYGSGGSS

Motif 3

RRAGHDRAAGS
RRAGHDRAAGS
RRAGHDRAAGS
RRAGHDRAAGS
RRAGHDRAAGS
RRAGHDRAAGS
RRAGHDRAAGS
RRAGHDSAAGS
RRAGHDSAAGS
RRAGHDSAAGS
RRAGHERAAGS
RRAGHGRSAGS

Motif 4

SGAGGAGGYGGYGGYGSYGSDS
SGAGGSGGYGGYGGYGGYGSDS
SGAGRSGGSYGWGDGGYGSDS
SGAGGSGGSYGWGDGGYGSDS
SGAGGSGGGYGWGDGGYGSDS
SGAGGSGGGYGWGDGGYGSDS
SGAGGSGGGYGWGDGGYGSDS
SGAGGSGGGYGWGDGGYGSDS
SGAGGSGGGYGWGDGGYGSDS
SGAGGSGGGYGWGDGGYGSDS
SGAGGSGGGYGWGDGGYGSDS
SGAGGAGGGYGWGDGGYGSDS
SGAGGAGGGYGWGDGGYSSDS
SGAGGSGGSYGWDYESYGSGS
SGAGGSGGYGGYGGYGSDS
SGAGGSGGYGGYGGYGSDS
SGAGGSGGYGGYGGYGSDS
SGAGGSGGYGGYGSDS
SGAGGSGGYGGYGSDS
SGAGGSGGYGGYGSDS
SGAGGSGGYGGYGSDS
SGAGGAGGYGGYGSDS
SGARGSGGYGGYGSDS
SGARGSGGYGGYGSDS
SGARGSGGYGGYGSDS

Motif 5

GSGAGGVGGGYGWGDGGYGSDS
GSGAGGVGGGYGWGDGGYGSDS
GSGAGGVGGGYGWGDGGYGSDS
GSGAGGVGGGYGWGDGGYGSDS
GSGAGGVGGGYGWGDGGYGSDS
GSGAGGVGGGYGWGDGGYGSDS
GSGAGGVGGGYGWGDGGYGSDS
GSGAGGRGGGYGWGDGGYGSDS
GSGAGGRGGGYGWGDGGYGSDS
GSGAGGSGGYGGYGGYGSDS
GSGAGGAGGYGGYGGYGSDS
GSGAGGRRGYGAYGSDSS
GSGAGGSGGYGGYGSDS
GSRRSGHDRAYGAGS

Figure 1. Gly-rich region of *Antheraea pernyi* silk fibroin partitioned into five motifs. Gray circles indicate the positive and negative charged amino acids.

monotonic rapid increase in *B. mori* silk fibroin fiber, but the slow increase with flat region like spider dragline silk in the silk fibers of three wild silkworms.[2,17,18] So it is important to study the structure and structural transition of the wild silkworms and compare it with the structural transition of *B. mori* silk fibroin. We studied previously both the solution- and solid-state structure of silk fibroin prepared from the silk gland of *S. c. ricini* silkworm as well as the silk fiber with NMR.[19−23] Since it is clear that the structural transition from α-helix to *β*-sheet occurs at the PLA region, the study has been concentrated at the PLA region. Our recent solid-state NMR study showed that the structural transition also occurs at the Gly-rich region with [1-^{13}C]Gly- or [^{15}N]Gly-labeled *S. c. ricini* silk fibroin samples.[23] It is interesting to study the structure and structural transition of the Gly-rich region in details during the α-helix to *β*-sheet transition of PLA domain. At first, the exact information on primary sequence of the Gly-rich region is required for the purpose. The amino acid composition of silk fibroin from *A. pernyi* is different from that of *B. mori* silk fibroin as shown in Table 1. The sum of Gly and Ala residues is 77%, which is basically the same as that of *B. mori* silk (73%), but the relative composition of Ala and Gly is reversed.[18] The proportion of Gly residues is greater

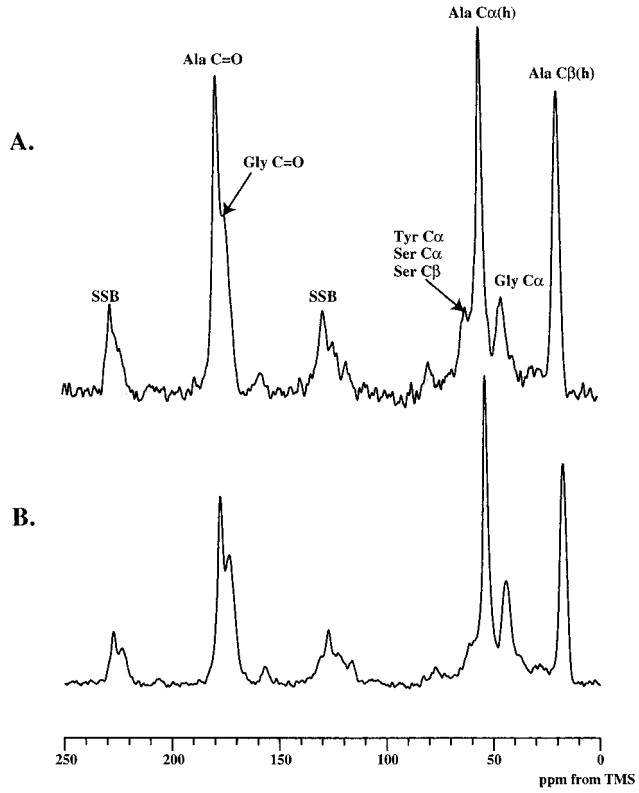

Figure 2. ^{13}C CP/MAS NMR spectra of natural abundance *Antheraea pernyi* (A) and *Samia cynthia ricini* (B) silk fibroin films. (h) denotes the α-helix conformation.

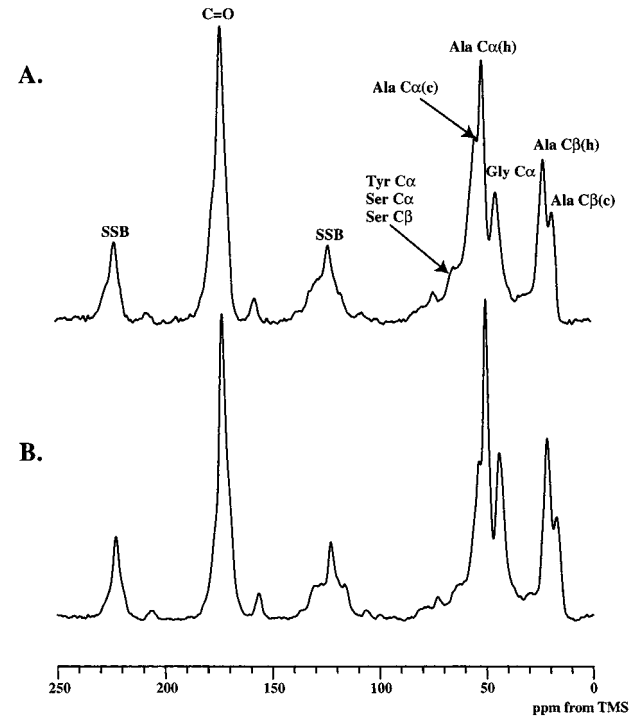

Figure 3. ^{13}C CP/MAS NMR spectra of natural abundance *Antheraea pernyi* (A) and *Samia cynthia ricini* (B) silk fibroin films after immersion in a 60% MeOH−water mixture for 90 min.

in *B. mori* silk fibroin, while the content of Ala residues is greater in *A. pernyi* silk fibroin. The complete sequence of the silk fibroin from *A. pernyi* has been determined by Yukuhiro et al.[24,25] The silk fibroin mainly consists of the repeated similar sequences by about 80 times where there are alternative appearances of the

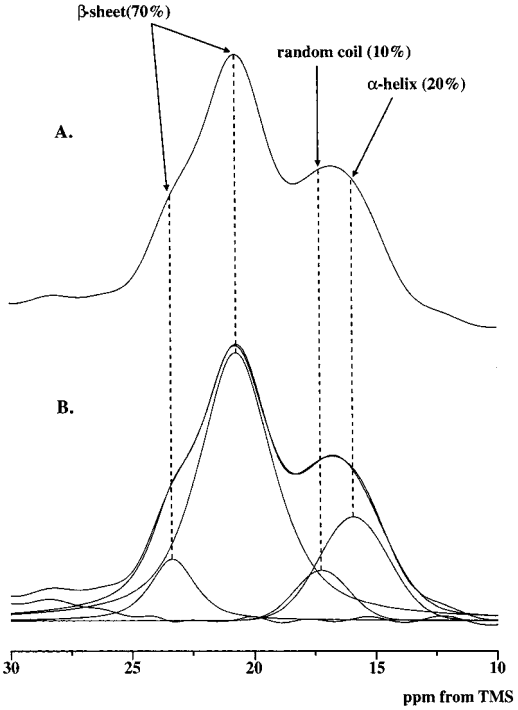

Figure 4. Expanded Ala C_β regions in ^{13}C CP/MAS NMR spectra of methanol-treated *Antheraea pernyi* silk fibroin film. The observed (A) and decomvoluted (B) spectra are shown.

poly(L-alanine) (PLA) region and the Gly-rich region like another wild silk worm, *S. c. ricini*[23,26] or spider (major ampullate) silk.[27,28] The Gly-rich region contains a variety of other amino acids as shown in Figure 1.

In this paper, the structure of silk fibroin prepared from the silk gland of *A. pernyi* is studied with ^{13}C CP/MAS NMR. For comparison, the ^{13}C CP/MAS NMR spectra of *S. c. ricini* silk fibroin will be observed. The selective ^{13}C isotope labeling of the Ser and Tyr residues in the Gly-rich region was performed. The isotropic ^{13}C chemical shifts of the C_α, C_β, and carbonyl carbons give us the conformation by using the empirical relationship between the conformation-dependent chemical shifts and the conformation or using chemical shift contour plots reported previously. The merits of ^{13}C NMR coupled with stable-isotope labeling of the sample give us the selective and detailed structural information without any degradation perturbation of the sample.

Materials and Methods

^{13}C Labeling of Silk Fibroin and Preparation of Silk Fibroin Film. *A. pernyi* larvae were reared in our laboratory. 100 μm of 10% (w/v) [2-^{13}C]Ser (99.9% ^{13}C enrichment, Mastrace, Inc., Woburn, MA) in aqueous solution was given by oral administration to fifth instar larvae from 3 to 6 old days for 4 days: two times, morning and evening, per day for a wild silkworm.[29,30] The middle silk gland was pulled out from an anesthetized 7-day-old fifth instar larva.[31] The silk glands containing [2-^{13}C]Ser silk fibroins were then washed twice in ice cold 1.15% potassium chloride solution. The center of the silk gland was cut, and the effluent was immersed in distilled water to remove the soluble protein, sericin. The most of sericin is removed by this treatment. The liquid silk that diluted with distilled water is extend to a plastic Petri dish and drying for 2 days to prepare the silk fibroin firm. Similarly, [3-^{13}C]Ser (99.9 at. % ^{13}C enrichment, Mastrace, Inc., Woburn, MA), [3-^{13}C]Tyr (99.9 at. % ^{13}C enrichment, Mastrace, Inc., Woburn, MA), and [1-^{13}C]Gly (99.9 at. % ^{13}C enrichment, Mastrace, Inc., Woburn, MA) were used to obtain [3-^{13}C]Ser, [3-^{13}C]Tyr, and [1-^{13}C]Gly *A. pernyi* silk fibroins, respectively. The liquid silk

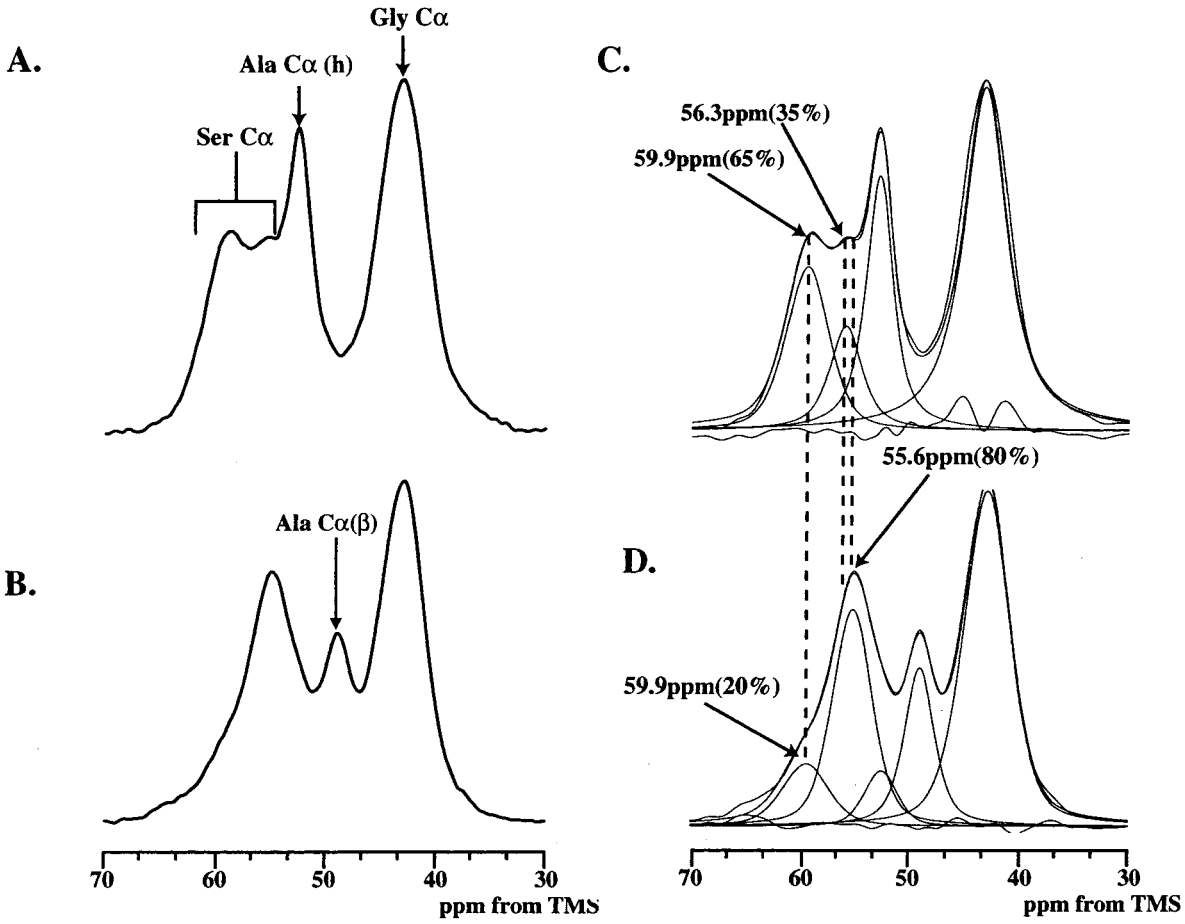

Figure 5. Expanded regions from 30 to 70 ppm in the ^{13}C CP/MAS NMR spectra of [2-^{13}C]Ser-labeled *Antheraea pernyi* silk fibroin films. The observed spectra, (A) and (B) of the sample without methanol treatment and the sample with immersion in 60% methanol−water treatment, respectively, are shown. The deconvoluted (C) and (D) spectra are also shown.

from *S. c. ricini* was also prepared for a comparison with the spectrum of *A. pernyi* silk fibroin.

NMR Observation. The ^{13}C CP/MAS NMR experiments were performed at 25 °C with CMX Infinity 400 NMR spectrometer (Chemagnetics) operating frequency of which was 100.04 MHz for ^{13}C nucleus. Samples were contained in a cylindrical rotor and spun at 3 kHz. The number of acquisitions was 8K, and the pulse delays were 3 s. A 50 kHz radio-frequency field strength was used for decoupling with a decoupling period of 12.8 ms. A 90° pulse width of 5 μs with 1 ms CP contact time was employed. Phase cycling was used to minimize artifacts. ^{13}C chemical shifts were calibrated indirectly through the adamantane methyl peak observed at 28.8 ppm relative to tetramethylsilane at 0 ppm.

Results and Discussion

^{13}C CP/MAS NMR Spectra of *A. pernyi* and *S. c. ricini* Silk Fibroins. Figure 2 shows natural abundance ^{13}C CP/MAS NMR spectra of *A. pernyi* and *S. c. ricini* silk fibroin films prepared from silk fibroins stored in the silk glands. Both spectra are remarkably similar. It is clear that PLA domains of both silk fibroins are mainly α-helix which is derived from the ^{13}C chemical shifts of Ala C_α, C_β, and C=O peaks: Ala C_α, 52.0 ppm; C_β, 15.8 ppm; and CO, 176.4 ppm.[8,12,13] The Ala C_β peak signifies that the main conformation is still α-helix although about 25% of Ala residues take a random coil (Figure 2). It is well-known that the α-helix in PLA domains of these silk fibroin films changes to β-sheet by stretching the films, by immersing them in organic solvents such as methanol or ethanol, and by hydration.[10,32] As an example, after immersing the films in 3:2 methanol−water mixture, the obseved ^{13}C CP/MAS spectra are shown in Figure 3. The spectra are considerably similar between *A. pernyi* and *S. c. ricini* silk fibroins. From the chemical shift change of the C_α, C_β, and C=O peaks of Ala residue, it is clear that the conformational transition from α-helix to β-sheet occurs at the PLA region although, some part of the PLA region still remains α-helix. To perform detailed conformational analysis, the C_β peak of Ala residue was expanded and decomposed, shown in Figure 4. From the decomposition of the peak by assuming the chemical shift values of Ala residue with α-helix, random coil, and β-sheet forms, the fraction is calculated as 20% α-helix, 10% random coil, and 70% β-sheet structures. The β-sheet peak has a shoulder at the low field site, which is a similar observation of Ala C_β region of *B. mori* silk fibroin. Thus, after the methanol−water treatment, the α-helix structure still remains in the PLA region. As shown in Figure 2, the number of Ala residues is almost constant, and therefore it is likely that part of a PLA domain takes both α-helix and β-sheet. The Ala residues with random coil form can be assigned to those in the Gly-rich domain rather than the PLA domain. However, it is difficult to clarify the conformation of other amino acid residues, and therefore, ^{13}C stable-isotope labeling of the silk fibroin samples seems useful for getting such information.

Analysis of Ser C_α Peak of [2-^{13}C]Ser *A. pernyi* Silk Fibroin. Figure 5 shows the expanded region (30−80 ppm) of ^{13}C CP/MAS NMR spectra of [2-^{13}C]Ser *A.*

Table 2. ^{13}C CP/MAS NMR Chemical Shifts of *A. pernyi* Silk Fibroin Film and Predicted Local Conformation along with the Fractions

		A. pernyi silk fibroin film				*A. pernyi* silk fibroin film with 60% MeOH treatment			
carbon in amino acids	random coil shifts (ppm)[33]	chemical shifts (ppm)	Δ (ppm)	conformation	fraction (%)	chemical shifts (ppm)	Δ (ppm	conformation	fraction (%)
Ala C_α	50.0	52.0	+2.0	α-helix		48.8	−1.2	*β*-sheet	
						52.0	+2.0	α-helix	
Ala C_β	16.6	15.8	+0.8	α-helix	75	15.6	−1.0	α-helix	10
		17.0	+0.4	random coil	25	17.1	+0.5	random coil	25
						20.0	+3.4	*β*-sheet	55
						22.9	+6.3	*β*-sheet	15
Ala C═O	175.5	176.4	+0.9	α-helix		171.9	−3.6	*β*-sheet	
Ser C_α	55.9	59.2	+3.3	α-helix	65	59.1	+3.2	α-helix	20
		55.6	−0.3	random coil	35	54.9	−1.0	*β*-sheet (including random coil)	80
Ser C_β	61.3	60.7	−0.6	α-helix	100	63.4	+2.1	*β*-sheet	60
						60.7	−0.6	α-helix (including random coil)	40
Tyr C_β	36.1	36.8	+0.7	random coil	100	36.8	+0.7	random coil	100
Gly C_α	42.7	43.1	+0.4	α-helix	100	42.8	−0.3	random coil	100
Gly C═O	171.3	172.3	+1.0	no prediction	100	170.9	−1.4	no prediction	100

pernyi silk fibroin before and after the 60% methanol−water mixture treatment. Table 2 summarizes the chemical shifts where random coil chemical shifts are also listed.[33] The transmutation between Ser and Gly residues is very active, and therefore the Gly C_α peak also become large, as reported previously.[34] The Ser C_α peak consists of two components: 55.6 ppm (random coil) and 59.2 ppm (α-helix), indicating the fractions are 35% and 65%, respectively. After a 3:2 methanol−water mixture treatment, the main peak of Ser C_α carbon was observed at 54.9 ppm assigned to the *β*-sheet. The α-helix peak at 59.2 ppm was observed as a shoulder of the main Ser C_α peak. The fraction is 80% *β*-sheet and 20% α-helix. The main C_β peak might include random coil peak although the latter component seems small. Thus, the ^{13}C stable isotope-labeled sample showed clearly that 65% of Ser residues take the α-helix in the silk fibroin film obtained from the silk gland and structural transition from the α-helix to *β*-sheet occur as well as the Ala residue. This means that 65% of the Ser residues are incorporated into the α-helix of the PLA region. It is very interesting that the most of Ser residues are localized at the N-terminal and C-terminal of PLA domain as shown in Figure 1. Thus, the Ser residue can be easily incorporated into the α-helix of PLA in silk fibroin in the silk gland. Then the conformation of such Ser residue will change to a *β*-sheet with structural transition of PLA by the 3:2 methanol−water treatment.

Analysis of Ser C_β Peak of [3-^{13}C]Ser *A. pernyi* Silk Fibroin. A similar analysis was performed for [3-^{13}C]Ser *A. pernyi* silk fibroin. The expanded spectra (30−80 ppm) in the ^{13}C CP/MAS NMR spectra of [3-^{13}C]-Ser *A. pernyi* silk fibroin before and after 3:2 methanol−water mixture treatments are shown in Figure 6. The spectra are quite different from Figure 5. In the case of the Ser C_β labeling, the increase of Gly C_α peak does not occur because the Ser C_β carbon does not contribute to the Gly C_α synthesis in silkworm although the amino acid transition from Ser to Gly residues occurs. The C_β peak of the Ser residue with *β*-sheet form appears at lower field than the α-helix peak contrary to the case of Ser C_α carbons, which are the same tendency to those of Ala residue. The chemical shift difference is small between the α-helix and random coil. Thus, the peak

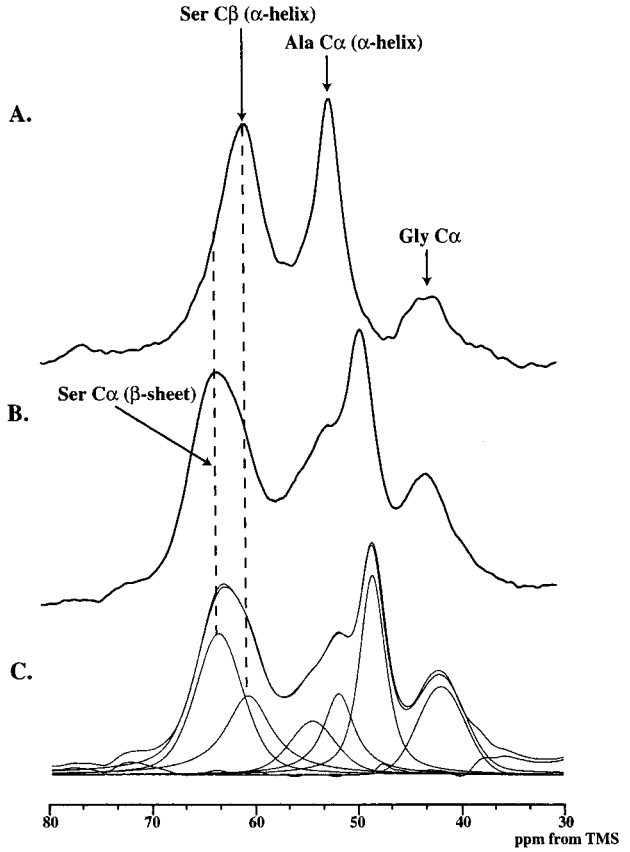

Figure 6. Expanded regions from 30 to 80 ppm in the ^{13}C CP/MAS NMR spectra of [3-^{13}C]Ser-labeled *Antheraea pernyi* silk fibroin films. The observed spectra, (A) and (B) of the sample without methanol treatment and the sample with immersion in 60% methanol−water treatment, respectively, are shown. The deconvoluted spectrum (C) of the spectrum (B) is also shown.

at 60.7 ppm is attributed to both α-helix and random coil structures, while the peak at 63.4 ppm is exclusively assigned to the *β*-sheet.

In the spectrum after methanol treatment, the fraction of *β*-sheet is calculated as 60% and sum of α-helix and random coil is 40%. Thus, the fraction of α-helix, random coil, and *β*-sheet of Ser residue is calculated

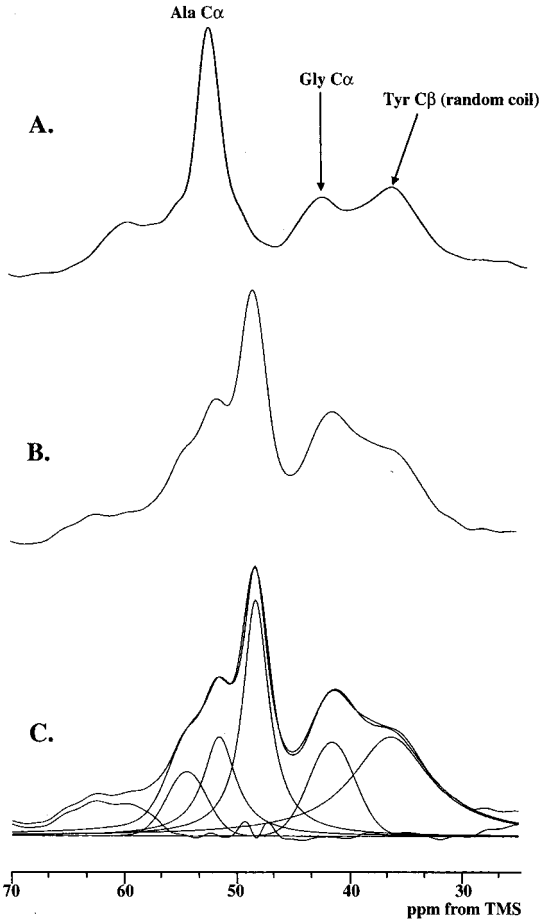

Figure 7. Expanded regions from 30 to 70 ppm in the ^{13}C CP/MAS NMR spectra of [3-^{13}C]Tyr-labeled *Antheraea pernyi* silk fibroin films. The observed spectra, (A) and (B) of the sample without methanol treatment and the sample with immersion in 60% methanol−water treatment, respectively, are shown. The deconvoluted spectrum (C) of the spectrum (B) is also shown.

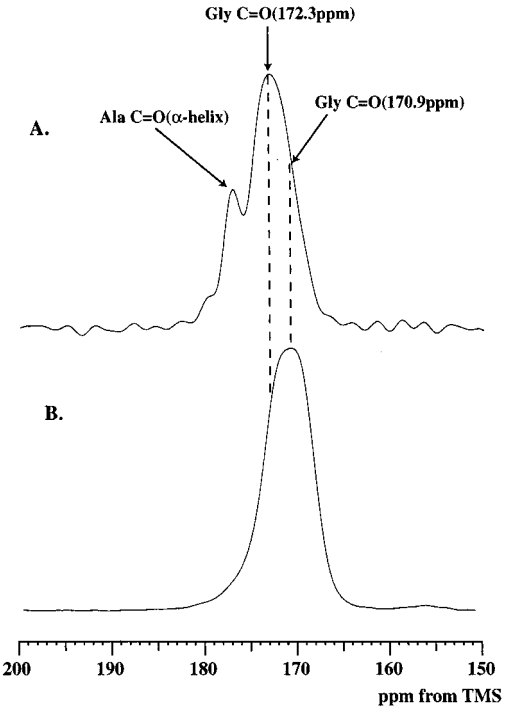

Figure 8. Expanded Gly C═O region in ^{13}C CP/MAS NMR spectra of [1-^{13}C]Gly-labeled *Antheraea pernyi* silk fibroin films. The observed spectra, (A) and (B) of the sample without methanol treatment and the sample with immersion in 60% methanol−water treatment, respectively, are shown.

from the spectra of [2-^{13}C]Ser and [3-^{13}C]Ser *A. pernyi* silk fibroins as 20% α-helix, 20%random coil, and 60% β-sheet for the 60% 3:2 methanol−water mixture treated silk fibroin film. The peak at 55 ppm is assigned to both natural abundance Ser C_α and Tyr C_β carbons.

Analysis of Tyr C_β Peak of [3-^{13}C]Tyr *A. pernyi* Silk Fibroin. The C_β peak of Tyr residue can be clearly observed in the ^{13}C CP/MAS NMR spectra of [3-^{13}C]Tyr *A. pernyi* silk fibroin (Figure 7). The peak position indicates that Tyr residue takes exclusively random-coil form. After methanol treatment, the main conformation is still random coil, although a small amount of Tyr residues might take the β-sheet. The increase of Gly C_α peak is considered due to the overlap with the tail of the main C_α peak of Ala residue with β-sheet.

Analysis of Gly C═O Peak of [1-^{13}C]Gly *A. pernyi* Silk Fibroin. A remarkable increase of the Gly carbonyl peak was observed in the ^{13}C CP/MAS NMR spectra of [1-^{13}C]Gly *A. pernyi* silk fibroin compared with natural abundance of the silk fibroin spectrum (Figures 2 and 8). The peak is broad and single. The natural abundance carbonyl peak from Ala residue with α-helix form is observed at the lower field. By immersing the silk fibroin film in 60% methanol, the ^{13}C CP/MAS NMR spectrum shift to higher field by 1.4 ppm although the peak was still broad. The carbonyl peak of Ala residue with β-sheet structure is also included in this single broad peak. This indicates that the structural transition also occurs in the Gly residues with structural change from α-helix to β-sheet of PLA region. In our previous paper, the ^{13}C CP NMR spectra of oriented [1-^{13}C]Gly *S. c. ricini*. silk fibroin fiber blocks were observed as a function of the angle between the fiber axis and magnetic field B_0. [23] The spectra changed significantly by changing the angles, and it was concluded that 65% of the Gly residue takes β-sheet structure as well as the Ala sequences. The proposed local structure of *A. pernyi* silk fibroin before and after methanol treatments for the motif 4 in Figure 1 is summarized in Figure 9.

Structural Analysis of the Gly-Rich Region for *A.pernyi* Silk Fibroin Based on the Conformational Parameters. The motif of the Gly-rich region of silk fibroin from *A. pernyi* is shown in Figure 1. The Gly-rich region can be divided into five different motifs. In motif 3, there are RGD sequences, which has cell adhesion properties.[35] In motifs 1, 4, and 5, the negatively charged amino acids are exclusively present in the C-terminal region of Gly-rich sequences, whereas the positively charged amino acids are present at the N-terminal region of Gly-rich sequences. The various naturally occurring amino acids differ in their intrinsic helical propensities. Statistical analysis of the frequency of occurrence of the natural amino acid with different side chains has distinct conformational preferences. Chou and Fasman have presented a secondary structure formation tendency of each amino acid, based on X-ray crystal structure data of many proteins statistically.[36−39] In other words, Chou and Fasman investigated the two frequencies: at first, they found the amino acid frequency that appears in the specific secondary structure and then the amino acid frequency compared with the frequency in the whole of the database. The relative parameters of each amino acid that appears in a particular secondary structures was determined. At

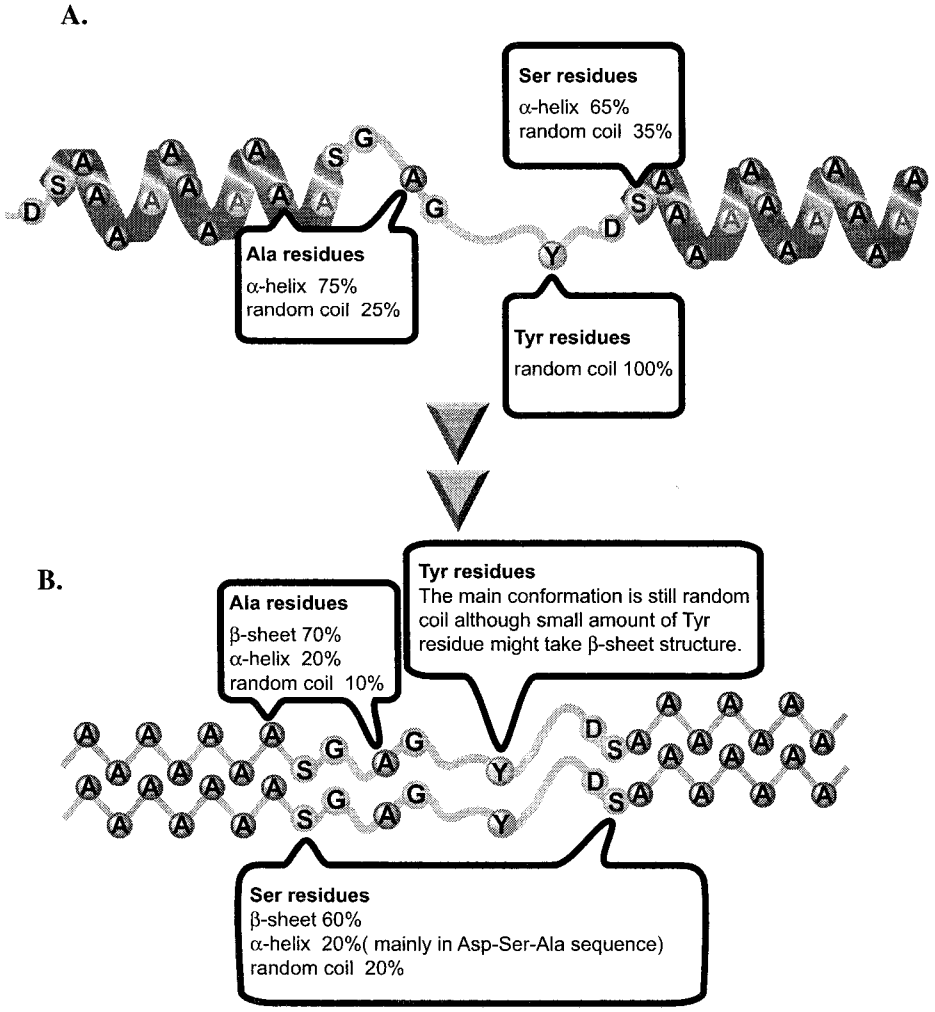

Figure 9. Scheme for the possible local structure of *Antheraea pernyi* silk fibroin films before (A) and after (B) 60% methanol−water treatment.

Table 3. Conformational Parameters of Several Amino Acids[36−39a]

amino acids	α-helix	β-sheet	$P_\alpha N$	$P_\alpha C$
Ala	**1.3−1.5**	**0.8−0.9**	**1.29**	**1.2**
Arg	**0.9−1.4**	**0.7−1.0**	**0.44**	**1.25**
Asn	0.8−0.9	0.6−0.7	0.81	0.59
Asp	**0.9−1.1**	**0.5−0.7**	**2.02**	**0.61**
Cys	0.9−1.0	0.8−1.2	0.66	1.11
Glu	1.4	0.5−0.8	2.44	1.24
Gln	1.1−1.4	0.8−1.0	1.22	1.22
Gly	**0.4−0.6**	**0.6−0.9**	**0.76**	**0.42**
His	1.0−1.2	0.8−1.1	0.73	1.77
Ile	1.0−1.1	1.5−1.8	0.67	0.98
Leu	1.3	1.0−1.2	0.58	1.13
Lys	1.1−1.2	0.7−0.9	0.66	1.83
Met	1.3−1.4	1.0−1.3	0.71	1.57
Phe	1.0−1.1	1.2−1.4	0.61	1.1
Pro	0.5−0.6	0.4−0.6	2.01	0
Ser	**0.7−0.8**	**0.9−1.0**	**0.74**	**0.96**
Thr	0.7−0.8	1.2−1.3	1.08	0.75
Trp	1	1.2	1.47	0.4
Tyr	0.7−0.9	1.2−1.5	0.68	0.73
Val	0.9−1.0	15−1.7	0.61	1.25

[a] $P_\alpha N$ and $P_\alpha C$ denote the probabilities of amino acid residues at α-helix border in N- and C-terminus, respectively. The bold letters mean the amino acid residues considered here.

present, this parameter is utilized to the various studies for structural biology, such as structural prediction[40] and helix capping.[41,42] Table 3 shows the conformational parameter of each amino acid and the probability of the amino acid residue which exists at the α-helix border in N- and C-terminals of proteins, respectively. The Ala residues have a high score in both α-helix and *β*-sheet structures, and thus, the Ala residue is highly susceptible to form both structures. So the PLA region in the silk fibroin film tends to form either α-helix or *β*-sheet. About Ser residue, 65% of the Ser residue was incorporated into α-helix structure of PLA region of the silk fibroin film before methanol treatment. From the values of the conformational parameters, PαN and PαC, by Chou and Fasman, Ser residue tends to present at both N- and C-terminals of the helical boundaries (Table 3). Therefore, it is speculated that the silk fibroin has prevented from the structural transition in the living body by arranging the Ser residue at the boundary region of α-helix structure. Furthermore, the Asp residue which is specifically arranged at the N-terminal of the α-helix structure of PLA domain has high score of α-helix as listed in Table 3. This also will be a stabilization factor of the α-helix structure because the Asp residue is close to the positive pole of the macrodipole, with α-helix and can make favorable charge−dipole interactions that stabilize the helix. The presence of the Asp-Ser sequence at the N-terminal in the silk fibroin film is speculated to is considered to take α-helix, and these arrangements of the primary structure are speculated to strengthen the α-helix of PLA domain. Actually, 20% of the Ser residues remains as α-helix in the silk fibroin film after methanol treatment. The fraction, 20%

of Ser residues is in agreement with the content of the Ser residue between Asp and Ala residues predicted from Figure 1.

Acknowledgment. T.A. acknowledges support from the Bio-oriented Technology Research Advancement Institution.

References and Notes

(1) Gosline, M. J.; Guerette, A. P.; Ortlepp, S. C.; Savage, N. K. *J. Exp. Biol.* **1999**, *202*, 3295−3303.
(2) Shimura, K. In *Zoku Kenshi no Kozo (Structure of Silk Fibers)*; Hojyo, N., Ed.; Shinshu University: Ueda, Japan, 1980; pp 335−352.
(3) Zhou, C.; Confalonieri, F.; Medina, N.; Zivanovic, Y.; Esnault, C.; Yang, T.; Jacquet, M.; Janin, J.; Duguet, M.; Perasso, R.; Li, Z. *Nucleic Acids Res.* **2000**, *28*, 2413−2419.
(4) Marsh, R. E.; Corey, R. B.; Pauling, L. *Biochim. Biophys. Acta* **1955**, *16*, 1−34.
(5) Fraser, R. D. B.; MacRae, T. P. In *Conformations of Fibrous Proteins and Related Synthetic Polypeptides*; Academic Press: New York, 1973.
(6) Takahashi, Y.; Gehoh, M.; Yuzuriha, K. *J. Polym. Sci., Polym. Phys. Ed.* **1991**, *29*, 889−891.
(7) Asakura, T.; Kuzuhara, A.; Tabeta, R.; Saito, H. *Macromolecules* **1985**, *18*, 1841−1845.
(8) Saito, H.; Iwanaga, Y.; Tabeta, R.; Narita, M.; Asakura, T. *Chem. Lett.* **1983**, 427−430.
(9) Saito, H.; Tabeta, R.; Asakura, T.; Iwanaga, Y.; Shoji, A.; Ozaki, T.; Ando, I. *Macromolecules* **1984**, *17*, 1405−1412.
(10) Ishida, M.; Asakura, T.; Yokoi, M.; Saito, H. *Macromolecules* **1990**, *23*, 88−94.
(11) Saito, H.; Ishida, M.; Yokoi, M.; Asakura, T. *Macromolecules* **1990**, *23*, 83−88.
(12) Asakura, T.; Demura, M.; Date, T.; Miyashita, M.; Ogawa, K.; Williamson, M. P. *Biopolymers* **1997**, *41*, 193−203.
(13) Asakura, T.; Iwadate, M.; Demura, M.; Williamson, M. P. *Int. J. Biol. Macromol.* **1991**, *24*, 167−171.
(14) Asakura, T.; Ashida, J.; Yamane, T.; Kameda, T.; Nakazawa, Y.; Ohgo, K.; Komatsu, K. *J. Mol. Biol.* **2001**, *306*, 291−305.
(15) Asakura, T.; Yamane, T.; Nakazawa, Y.; Kameda, T.; Ando, K. *Biopolymers* **2001**, *58*, 521−525.
(16) Asakura, T.; Ashida, J.; Yamane, T. *ACS Books*, in press.
(17) Vollrath, F.; Knight, D. P. *Nature (London)* **2001**, *410*, 541−548.
(18) Iizuka, E. In *Zoku Kenshi no Kozo (Structure of Silk Fibers)*; Hojyo, N., Ed.; Shinshu University: Ueda, Japan, 1980; pp 165−174.
(19) Asakura, T.; Murakami, T. *Macromolecules* **1985**, *18*, 2614−2619.
(20) Asakura, T.; Kashiba, H.; Yoshimizu, H. *Macromolecules* **1988**, *21*, 644−648.
(21) Asakura, T.; Yoshimizu, H.; Yoshizawa, F. *Macromolecules* **1988**, *21*, 2038−2041.
(22) Nakazawa, Y.; Nakai, T.; Kameda, T.; Asakura, T. *Chem. Phys. Lett.* **1999**, *311*, 362−366.
(23) Asakura, T.; Ito, T.; Okudaira, M.; Kameda, T. *Macromolecules* **1999**, *32*, 4940−4946.
(24) Yukuhiro, K.; Kanda, T.; Tamura, T. *Insect Mol. Biol.* **1997**, *6*, 89−95.
(25) Sezutsu, H.; Yukuhiro, K. *J. Mol. Evol.* **2000**, *51*, 329−338.
(26) Personal communication.
(27) Simmons, A. H.; Michal, C. A.; Jelinski, L. W. *Science* **1996**, *271*, 84−87.
(28) Xu, M.; Lewis, R. V. *Proc. Natl. Acad. Sci. U.S.A.* **1990**, *87*, 7120−7124.
(29) Asakura, T.; Kawaguchi, Y.; Demura, M.; Osanai, M. *Insect Biochem.* **1988**, *18*, 531−538.
(30) Asakura, T.; Suzuki, H.; Tanaka, T. *J. Seric. Sci. Jpn.* **1985**, *54*, 504−509.
(31) Asakura, T.; Suzuki, H.; Watanabe, Y. *Macromolecules* **1983**, *16*, 1024−1026.
(32) Tsukada, M.; Freddi, G.; Monti, P.; Bertoluzza, A. *J. Polym. Sci., Polym Phys. Ed.* **1995**, *33*, 1995−2001.
(33) Asakura, T.; Watanabe, Y.; Uchida, A.; Minagawa, H. *Macromolecules* **1984**, *17*, 1075−1081.
(34) Wareick, S. *J. Biol. Chem.* **1949**, *178*, 519−520.
(35) Pierschbacher, M. D.; Ruoslahti, E. *Nature (London)* **1984**, *309*, 30−33.
(36) Chou, P. Y.; Fasman, D. G. *Annu. Rev. Biochem.* **1978**, *47*, 251−276.
(37) Chou, P. Y.; Fasman, D. G. *Adv. Enzymol.* **1978**, *47*, 45−148.
(38) Chou, P. Y. In *Prediction of Protein Structure and the Principles of Protein Conformation*; Fasman, D. G., Ed.; New York, 1989; pp 549−586.
(39) Chou, P. Y.; Fasman, D. G. *J. Mol. Biol.* **1977**, *115*, 135−175.
(40) Bystroff, C.; Thorsson, V.; Baker, D. *J. Mol. Biol.* **2000**, *301*, 173−190.
(41) Aurora, R.; Rose, G. D. *Protein Sci.* **1998**, *7*, 21−38.
(42) Richardson, J. S.; Richardson, D. C. *Science* **1988**, *240*, 1648−1652.

MA011999T